Analytic Efficiency Optimization of Solar Cells under Light Concentration in the Framework of the Single-Diode Model

Rolf Brendel

Herein, concentrating solar cells are modeled with two recombination active contacts and a recombination active light absorber in the framework of the one-diode model. The two contacts and the absorber contribute to a lumped series resistance and to a lumped recombination current. It is proven that varying the light concentration can be interpreted as iso-selectivity scaling of the cell's resistance and the cell's recombination. As a consequence of that, the optimal efficiency of a concentrator cell is found at maximum combined selectivity of the two contacts and the absorber. Herein, analytic formulas are derived that calculate the optimal contact areas and the optimal light concentration level for achieving an optimum efficiency. The resulting formulas express the efficiency in terms of the selectivities of each contact and the selectivity of the absorber. These equations are used to calculate the optimum contact area fractions and the optimum light concentration level for Si solar cells of various material qualities with screen-printed Al-doped contacts and n-type poly-Si contacts on oxide. The efficiency results of the novel analytic and a conventional numeric optimization agree to the expected level of accuracy.

1. Introduction

Solar cells are typically modeled using well-established numerical device simulations that go far beyond the simple one-diode model. However, simplifying and even over-simplifying treatments are also of interest as they allow quick estimates of appropriate device designs with little effort. Our screening of cell designs with various nonideal contact combinations was done in the framework of the one-diode model and may serve as an example for this: we identified a combination of poly-Si contacts with amorphous Si contacts

as the highest performing combination for crystalline Si solar cells.[1] With a purely analytic approach using the one-diode model, we also found that poly-Si junctions in combination with conventional screen-printed Al contacts allow high efficiencies with least changes relative to the proven passivating emitter rear contact technology.[2] As a result of this, we are now investigating this type of solar cells experimentally.[3] However, our previous analytic modeling did not consider extrinsic recombination losses in the bulk of the absorber and did also not consider light concentration. Rau and Kirchartz recently presented an analytical equation for the optimal device efficiency in the framework of the one-diode model.[4] Their work did also not account for arbitrary bulk recombination. Until now, there is apparently no analytic one-diode model for the optimal solar cell efficiency with partial nonideal contacts and arbitrary bulk recombination current.

This paper closes this gap and generalizes previous treatments to light concentrating cells. We start with basic assumptions and generalized definitions and then prove that varying the level of light concentration is an iso-selectivity scaling that balances a cells recombination against its resistance. From previous work, we know that a cell that allows for iso-selectivity scaling exhibits its maximum efficiency at maximum selectivity[4,5] and that this maximum selectivity can easily be calculated for given contact parameters.[5] Combining these previous findings with the recent analytic efficiency expression from ref. [4] we derive new formulas for the optimal contact fractions, the optimal light concentration, and the resulting optimal cell efficiency. Some of these formulas are surprisingly simple.

For testing the analytic treatment against a numeric optimization, we apply the new formulas to calculating the contact area fractions and the optimum light concentration factors for the so-called poly-Si on oxide (POLO) Si solar cells[6] that combine screen-printed Al-doped contacts with n-type POLO.[1]

2. Assumptions and Definitions

2.1. Current–Voltage Curve and Selectivities

A solar cell's ideal diode equation describes the current density

$$J(V) = J_{sc} - J_c\left(e^{\frac{V+J\rho_c}{nV_{th}}} - 1\right) \tag{1}$$

R. Brendel
Institute for Solar Energy Research Hamelin (ISFH)
Am Ohrberg 1, 31860 Emmerthal, Germany
E-mail: brendel@isfh.de

R. Brendel
Institute for Solid State Physics
Leibniz University Hannover
Appelstrase 2, 30167 Hannover, Germany

The ORCID identification number(s) for the author(s) of this article can be found under https://doi.org/10.1002/solr.202300279.

as a function of the terminal voltage V. The cell's recombination current density is J_c and the ideality factor is n. The series resistance is ρ_c and the 1-sun short-circuit current density is J_{sc}. The wide use of one- and two-diode models for quantitatively describing measured current–voltage curves of solar cells[7] underlines the practical relevance of this simple modeling approach. Here, we consider a one-diode model without a shunt resistance. This is valid for good solar cells. The red lines in **Figure 1** show efficiencies

$$\eta = \max_V \left(\frac{V J(V)}{P_{\mathrm{in,1sun}}} \right) \quad (2)$$

that we calculate numerically for any given point (ρ_c, J_c) by varying the terminal voltage V to find the maximum efficiency η. The numerical values for J_{sc}, the thermal voltage V_{th}, the ideality n, and the 1-sun insulation power $P_{\mathrm{in,1sun}}$ are given in the caption of Figure 1 and are taken from ref. [8].

The ideal diode Equation (1) is an approximation that describes real cells the better, the more flat the quasi Fermi levels are. For flat quasi Fermi levels, all recombination processes are running at the same internal voltage $V + J\rho_c$.

In the framework of the one-diode model, we consider the cell's lumped resistance

$$\rho_c = \rho_a + \rho_e/f_e + \rho_h/f_h \quad (3)$$

and the cell's lumped recombination current density

$$J_c = J_a + f_e J_e + f_h J_h \quad (4)$$

to be made up of contributions from the absorber a, the electron contact e, and the hole contact h, respectively. Reduced area fractions f_e and $f_h < 1$ of small-scale contacts enhance the series

resistance contributions and reduce the recombination current contributions, respectively. The noncontacted area is assumed to be insulating and free of recombination. Note that for a noncontacted surface with recombination current $J_s > 0$, we may still use the later presented results when considering $(f_e J_e - J_s)/(J_e - J_s) \geq 0$ rather than f_e as the physical electron contact fraction. A corresponding relation holds for the hole-contacted side of the cell. Area fractions f_e and $f_h > 1$ can be interpreted as a small-scale roughening of the respective full-area surfaces. In both cases, the term "small scale" shall permit the use of unique internal voltage anywhere in the device. Please note that Equation (1) also implies that all recombination processes exhibit the same ideality factor n.

We define the selectivity

$$S_x = \frac{n V_{th}}{J_x \rho_x} \quad (5)$$

for the whole cell ($x = c$), the electron contact ($x = e$), the hole contact ($x = h$), and the absorber ($x = a$). We do this in formal analogy to our previous definition of the selectivity of a cell's contact[5] while generalizing the previous definition to non-unity ideality factors n. The selectivities S_x can have large numeric values. We therefore define their logarithms to the base 10

$$S_{10,x} = \log(S_x) \quad (6)$$

and to the base e

$$S_{\exp,x} = \ln(S_x) \quad (7)$$

For any recombination current J_x, we define a conjugated recombination resistance

$$\tilde{\rho}_x = n V_{th}/J_x \quad (8)$$

representing a resistance that minority carriers have to overcome for recombination. Similarly, we define a conjugated transport current density

$$\tilde{J}_x = n V_{th}/\rho_x \quad (9)$$

for any transport resistance ρ_x that characterizes the current density that flows across this resistance at thermal voltage. The previously defined selectivities may thus be written as

$$S_x = \frac{\tilde{J}_x}{J_x} = \frac{\tilde{\rho}_x}{\rho_x} \quad (10)$$

This equation was in fact the physical motivation for the selectivity definition (5) when first applied to contacts:[5] for the majority carriers, recombination at the contact and transport through the contact are two alternative processes. We defined the contact selectivity S_x with ($x = e, h$) as the ratio of the wanted process—a majority carrier current $\tilde{J}_x$ through the contact resistance ρ_x—and the unwanted process—majority carrier recombination by a recombination current J_x with a resistance $\tilde{\rho}_x$ against recombination.
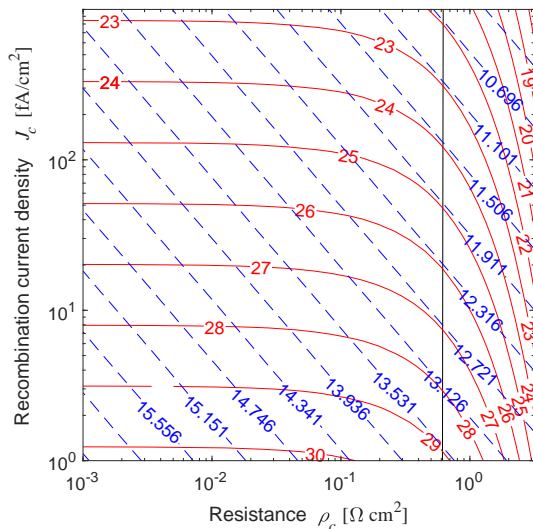

Figure 1. Solid red lines: iso-lines of the energy conversion efficiency from numerically finding the maximum efficiency (Equation (2)) for short-circuit current density $(J_{sc}) = 43.48 \, \mathrm{mA \, cm^{-2}}$, $n = 1$, $V_{th} = 25.68 \, \mathrm{mV}$, and $P_{\mathrm{in,1sun}} = 1000 \, \mathrm{W \, m^{-2}}$. Broken blue lines: iso-lines of the selectivity $S_{10,c}$ calculated with Equation (16) for the efficiency values of the red lines. Black solid line: magic resistance $\rho_c = \rho_m$ coding to Equation (12).

2.2. Inverse Scaling of Recombination and Resistance

Let us now assume without reference to a physical interpretation that J_c and ρ_c are not independent but can be scaled inversely: reducing the recombination current density to a fraction $f_c J_c$ with $f_c < 1$ shall enhance the device-effective transport resistance to ρ_c/f_c. The scaled device-effective selectivity $S_c = \frac{n V_{th}}{(f_c J_c)(\rho_c/f_c)}$ is then invariant under scaling. Scaling does, however, make a difference to the efficiency of the solar cell because varying f_c deliberately balances recombination losses against resistive losses. The physical interpretation will follow Section 3.2.

2.3. Magic Resistance for Optimal Inverse Scaling

In ref. [5], we showed numerically that for any pair of parameters (J_c, ρ_c), the optimal inverse scaling $(f_c J_c, \rho_c/f_c)$ maximizing the efficiency is

$$\rho_c/f_c = \rho_m = 0.61\,\Omega\,cm^2 \tag{11}$$

when using the parameters given in the caption of Figure 1. Here, the index m in ρ_m stands for magic resistance as it is on the first glance quite surprising to find this resistance being independent of the contacts recombination current J_c. Rau and Kirchartz disenchanted this magic by proving analytically that Equation (11) is in good approximation with a property of the diode Equation (1).[4] Following their derivation and allowing for nonunity ideality, we find

$$\rho_m = n V_{th}/J_{sc} \tag{12}$$

The solid black line in Figure 1 shows $\rho_c = \rho_m$.

2.4. Parameters of the Illuminated Current–Voltage Curve under Optimal Inverse Scaling

Following the analytical treatment in ref. [4], the open-circuit voltage at optimal scaling is

$$V_{oc} = n V_{th} S_{exp,c} \tag{13}$$

and is thus independent of the J_{sc}. Inserting this into Green's approximation for the prefactor of the fill factor[9] gives

$$FF_0(S_{exp,c}) = \frac{S_{exp,c} - \ln(S_{exp,c} + 0.72)}{S_{exp,c} + 1} \tag{14}$$

This prefactor is thus a sole function of the selectivity $S_{exp,c}$. The efficiency[4]

$$\eta = \frac{j_{sc} n V_{th}}{P_{in}} (S_{exp,c} - 1) FF_0(S_{exp,c}) \tag{15}$$

thus depends only on the selectivity $S_{exp,c}$ once the J_{sc}, the input power density P_{in}, and the ideality n are set. The analytic results (12) through (15) rely on analytical approximations for the fill factor and neglect the derivative of the fill factor versus the scaling factor f_c. This makes the results approximations. In ref. [4], the efficiency (15) was tested to overestimate the correct result by

0.05%, corresponding to an error of the order of $0.1\%_{abs}$ efficiency points for silicon cells.

Using $S_{exp,c} = \ln(10) S_{10,c}$ and Taylor expanding (15) around $S_{10,c} = 13$ yields to the first order in $(S_{10,c} - 13)$ the efficiency

$$\eta = \frac{j_{sc} n V_{th}}{P_{in}} (2.21104 S_{10,c} - 3.94672) \tag{16}$$

at optimum scaling. Equation (16) is equivalent to $\eta/\% = 2.46895 S_{10,c} - 4.40715$ for the parameters given in the caption of Figure 1. This is very similar to the $\eta/\% = 2.4733 S_{10,c} - 4.432$ as derived from a numerical optimization in ref. [5]. The deviations of these two efficiencies are again of the order of $\Delta \eta = 0.1\%_{abs}$. We use (16) with the parameter values given in the caption of Figure 1 to calculate the selectivities $S_{10,c}$ that correspond to the efficiency values η of the red iso-efficiency lines in Figure 1. These iso-selectivity lines are plotted broken and in blue in Figure 1. They should be tangent to the iso-efficiency lines at $\rho_c = \rho_m$. The slope at $\rho_c = \rho_m$ is as expected. However, the values deviate by about $\Delta \eta = 0.1\%$ efficiency points due to the limited accuracy of the analytic calculation (15).

The efficiency of any solar cell obeying the ideal diode Equation (1) with arbitrary ideality factor n can thus be optimized by iso-selectivity scaling.[4,5] Inverse scaling of J_c and ρ_c with a factor $f = \rho_c/\rho_m$ yields the optimum efficiency that can be calculated with (15) or with the linearization (16).

3. Maximizing the Device Efficiency

3.1. Maximizing the Selectivity

Maximizing S_c with respect to f_e and f_h by using (5), (3), and (4) requires solving the equation system $\frac{\partial S_c}{\partial f_e} = 0 \wedge \frac{\partial S_c}{\partial f_h} = 0$. The solution is

$$f_e = \frac{\sqrt{\rho_e \tilde{\rho}_e}}{\sqrt{\rho_a \tilde{\rho}_a}} = \sqrt{\frac{J_a \rho_e}{J_e \rho_a}} \quad \wedge \quad f_h = \frac{\sqrt{\rho_h \tilde{\rho}_h}}{\sqrt{\rho_a \tilde{\rho}_a}} = \sqrt{\frac{J_a \rho_h}{J_h \rho_a}} \tag{17}$$

and it follows

$$\frac{f_e}{f_h} = \sqrt{\frac{J_h \rho_e}{J_e \rho_h}} \tag{18}$$

The optimal ratio of the contact areas can thus be deduced from the contact properties only. It is independent of the absorber properties. With the selectivity-maximizing fractions (17), the total cell resistance at optimum selectivity is

$$\rho_c = \sqrt{\rho_a \tilde{\rho}_a} \left(\frac{1}{\sqrt{S_a}} + \frac{1}{\sqrt{S_e}} + \frac{1}{\sqrt{S_h}} \right) \tag{19}$$

and the total recombination current density becomes

$$J_c = \sqrt{J_a \tilde{J}_a} \left(\frac{1}{\sqrt{S_a}} + \frac{1}{\sqrt{S_e}} + \frac{1}{\sqrt{S_h}} \right) \tag{20}$$

Here, we use the conjugated recombination resistance $\tilde{\rho}_a$ of the absorber and the conjugated transport current density $\tilde{J}_a$

of the absorber in the latter two equations for achieving an easy-to-remember notation. Multiplying the left- and right-hand sides of (19) and (20), respectively, and using $J_x \tilde{\rho}_x = \tilde{J}_x \rho_x = nV_{th}$, we find that the relation

$$\frac{1}{\sqrt{S_c}} = \frac{1}{\sqrt{S_a}} + \frac{1}{\sqrt{S_e}} + \frac{1}{\sqrt{S_h}} \quad (21)$$

giving the maximum achievable selectivity S_c as a function of the selectivities of the contacts and the absorber.

3.2. Maximizing the Efficiency of a Concentrator Cell

Equations (19) and (20) define a point (ρ_c, J_c) in Figure 1 on the S_c iso-line of maximum selectivity. Using the scaling factor

$$f_c = \frac{\rho_c}{\rho_m} \quad (22)$$

from (11) and (12) brings the cell to maximum efficiency at $(\rho_c/f_c, f_c J_c)$ under the constraint of constant selectivity. From (19), we find the efficiency-maximizing scaling factor

$$f_c = \frac{\sqrt{\rho_a \tilde{\rho}_a}}{\rho_m} \left(\frac{1}{\sqrt{S_a}} + \frac{1}{\sqrt{S_e}} + \frac{1}{\sqrt{S_h}} \right) \quad (23)$$

The maximum efficiency directly follows from (15) or (16) when using S_c from (21).

We now give a physical interpretation of this efficiency-maximizing scaling factor f_c. The scaled solar cell has the efficiency η defined by the equations

$$\eta = \max_V \left(\frac{VJ(V)}{P_{in,1sun}} \right) \quad \wedge \quad J(V) = J_{sc} - f_c J_c \left(e^{\frac{V + J(\rho_c/f_c)}{nV_{th}}} - 1 \right) \quad (24)$$

Expanding the first part of (24) and multiplying the second part by the factor

$$C = 1/f_c \quad (25)$$

respectively, we find

$$\eta = \max_V \left(\frac{VCJ(V)}{CP_{in,1sun}} \right) \quad \wedge \quad CJ(V) = CJ_{sc} - J_c \left(e^{\frac{V + CJ\rho_c}{nV_{th}}} - 1 \right) \quad (26)$$

Renaming the variable $CJ(V) \rightarrow J(V)$ and using $CP_{in,1sun} = P_{in,Csuns}$, this transforms to

$$\eta = \max_V \left(\frac{VJ(V)}{P_{in,Csuns}} \right) \quad \wedge \quad J(V) = CJ_{sc} - J_c \left(e^{\frac{V + J\rho_c}{nV_{th}}} - 1 \right) \quad (27)$$

The latter equation system describes the efficiency of the non-scaled cell under light concentration C. The linear scaling of ρ_c and J_c by the factor f_c has the physical interpretation of putting the device under concentration $C = 1/f_c$. Equations (25) and (23) can thus be used to calculate the optimal light concentration level that maximizes the efficiency for a cell with optimal contact area fractions.

3.3. Maximizing the Efficiency of a Non-Concentrating Cell

Scaling a device with maximized selectivity to the point of maximum efficiency is not possible for a non-concentrating cell. Non-concentrating cells will typically have an optimum efficiency at contact fractions f_e and f_h with less than maximum selectivity. Here, we report the contact fractions that maximize the efficiency in this case.

Using Equation (S21), of the supplementary information of ref. [4], we find the cells efficiency

$$\eta = \left(nv_t \ln \left(\frac{J_{sc}}{J_a + f_e J_e + f_h J_h} \right) J_{sc} - \left(\rho_a + \frac{\rho_e}{f_e} + \frac{\rho_h}{f_h} \right) J_{sc}^2 \right) FF_0 / P_{in,1sun} \quad (28)$$

as the product of open-circuit voltage, the approximate fill factor and the J_{sc}. We then find the contact fractions for maximum efficiency by solving the equation system $\frac{\partial P_{out}}{\partial f_e} = 0 \quad \wedge \quad \frac{\partial P_{out}}{\partial f_h} = 0$. Here $P_{out} = VJ(V)$ is the output power delivered by the solar cell. The contact area fractions follow from solving two equations that are quadratic in f_e and f_h, respectively, and by selecting the positive solutions

$$f_e = \frac{1}{2} \frac{J_{sc}}{\sqrt{J_e J_e}} \left(\frac{1}{\sqrt{S_e}} + \frac{1}{\sqrt{S_h}} + \sqrt{\left(\frac{1}{\sqrt{S_e}} + \frac{1}{\sqrt{S_h}} \right)^2 + 4\frac{J_a}{J_{sc}}} \right) \wedge$$
$$f_h = \frac{1}{2} \frac{J_{sc}}{\sqrt{J_h J_h}} \left(\frac{1}{\sqrt{S_e}} + \frac{1}{\sqrt{S_h}} + \sqrt{\left(\frac{1}{\sqrt{S_e}} + \frac{1}{\sqrt{S_h}} \right)^2 + 4\frac{J_a}{J_{sc}}} \right). \quad (29)$$

Inserting this in (28), we find the maximum efficiency under 1 sun. Note that the ratio of hole to electron contact area fraction f_e/f_h given by Equation (18) also follows from (29) and is thus the same for the concentrating and the non-concentrating case. Again, the results of this section are approximations because (28) is an approximation and because finding the maximum power point neglected the voltage dependence of FF_0.[4]

3.4. Test and Application of the Analytic Treatment

For testing the analytic one-diode model equations against the numeric solutions, we consider a POLO solar cell with a p-type Si wafer of resistivity 1 Ωcm, a wafer thickness $W = 150\,\mu m$, and a $J_{sc} = 42\,mA\,cm^{-2}$. The cell shall have a passivating poly-silicon electron-selective contact with $J_e = 3\,fA\,cm^{-2}$ and a recombination active local screen-printed Al-doped hole-selective contact with a recombination current density of $J_h = 500\,fA\,cm^{-2}$. The two contact resistances shall be $\rho_e = \rho_h = 1\,m\Omega cm^2$. These values are typical for the contacts of POLO cells.[6] We vary the recombination parameter J_a of the absorber in a wide range from 1 to 1000 fA cm^{-2} and consider three absorber resistances $\rho_a = 10$, 100, and 500 mΩcm^2.

Figure 2 shows the testing for 1 sun illumination. The analytic optimum contract area fractions (29) and efficiencies (28) are shown as broad dashed lines. According to (29), the contact area fractions do not depend on the series resistance of the absorber. This is why the blue-dashed line for $\rho_a = 500\,m\Omega cm^2$ hides the lines of the two other resistances. Numerically maximizing the efficiency (27) for fixed $C = 1$ is a three-parameter optimization
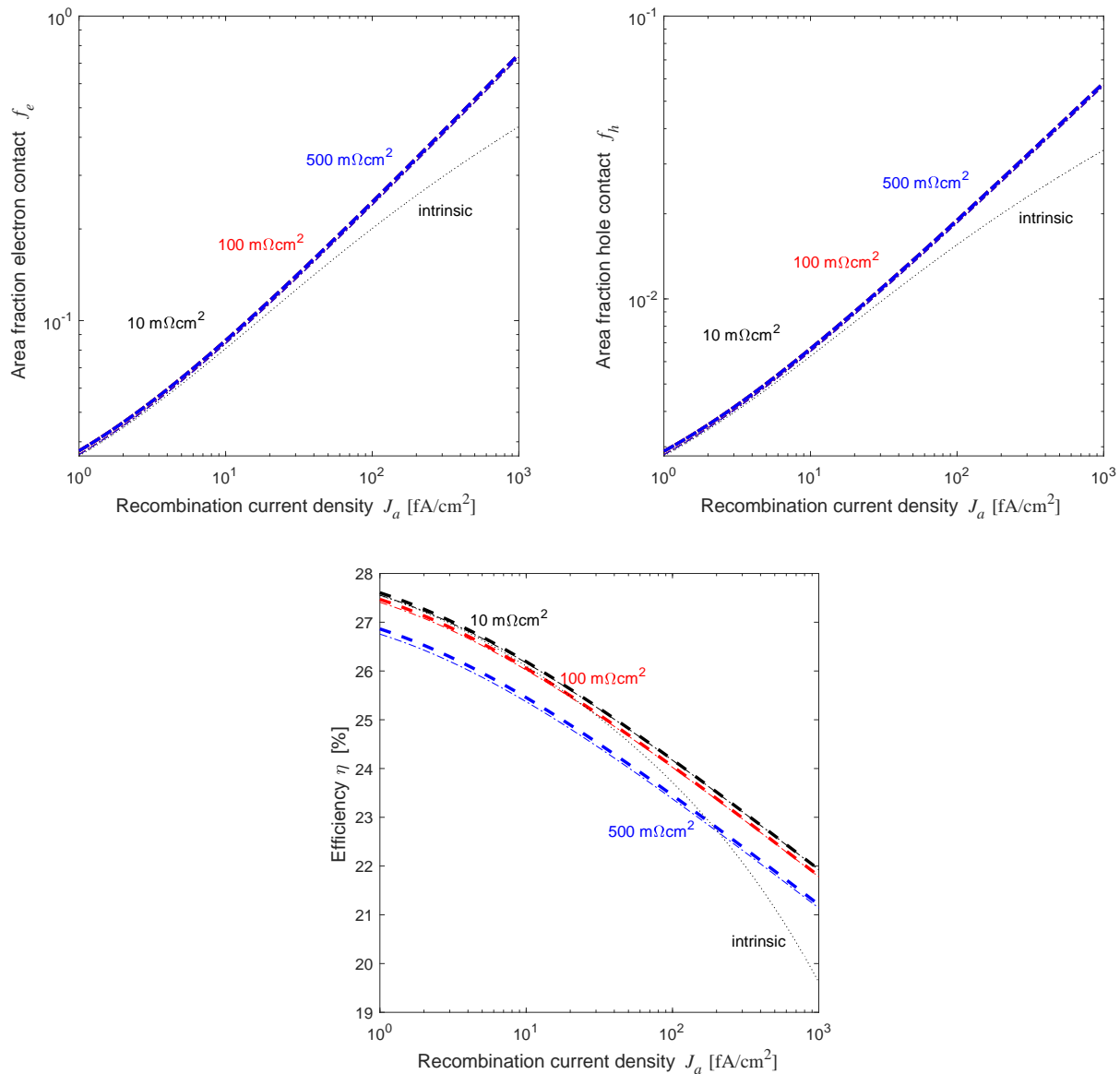
Figure 2. Comparison of analytic and numeric optimization under 1 sun illumination. The colors distinguish different absorber resistances ρ_a. Broad dashed lines: analytical results for the area fractions of the electron contact f_e (top left graph) and the hole contact f_h (top right graph) from Equation (29), and efficiency η (bottom graph) from (28). Narrow dash-dotted lines: results of the numeric optimization. The parameters are $J_{sc} = 42$ mA cm^{-2}, $n = 1$, $V_{th} = 25.68$ mV, $P_{in,1sun} = 1000$ W m^{-2}, $\rho_e = \rho_h = 1$ mΩcm, $J_e = 3$ fA cm^{-2}, and $J_h = 500$ fA cm^{-2}. Dotted lines: numeric optimization applying the injection-dependent intrinsic resistance ρ_a of the absorber that is calculated numerically at the maximum power point for a p-type 1 Ωcm Si wafer with a thickness $W = 150$ μm.

of f_e, f_h, and of the terminal voltage V. The voltage is optimized to find the maximum power point. The numeric results are plotted as narrow dash-dotted lines in Figure 2. They deviate from the analytic result by about 0.08%$_{abs}$ efficiency points. The dotted black line is calculated numerically and applies an injection-dependent intrinsic series resistance of the Si wafer that follows from the algorithms described in ref. [8] when assuming spatially homogeneous photo generation.

Figure 3 shows the respective testing for optimized light concentration C. The broad dashed lines are the analytical results for the contact area fractions from (17), the light concentration from

(25) and (22), and the efficiency from (15). Searching the optimum efficiency numerically with (27) is a four parameter optimization of f_e, f_h, $C = 1/f_c$, and V. The numeric results are shown as narrow dash-dotted lines. The perfect agreement of analytic and numeric contact fractions is due to not making any approximations when deriving the analytic formula (21) that maximize the selectivity. We find electron contact area fractions that are always a factor of 12.9 larger than that for the holes from (18) when inserting the specific contact parameters. The deviation between numeric and analytic optimal light concentration C is 4%. Some deviation is expected because the analytic formulas
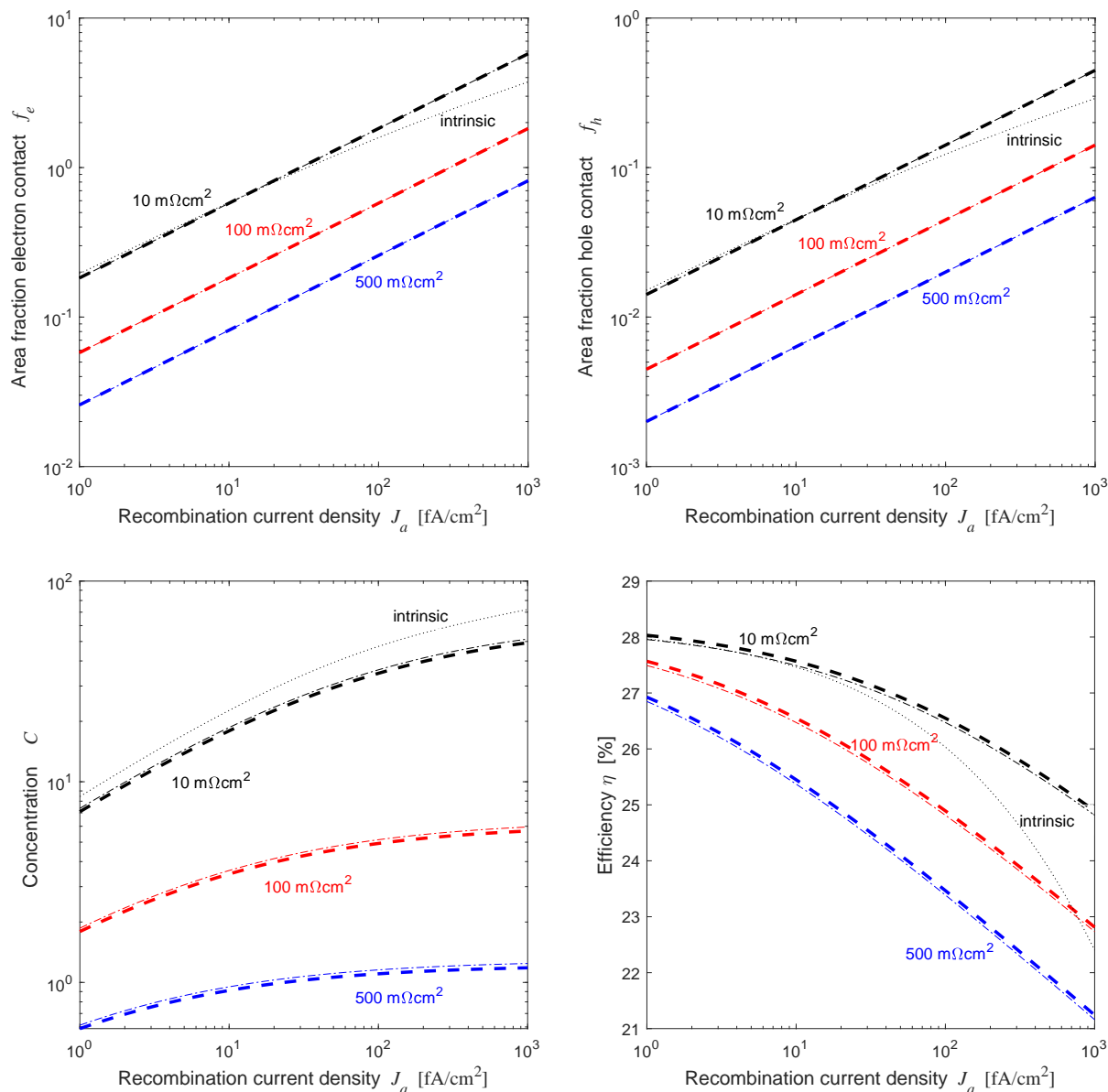
2300279 (5 of 7)

Figure 3. Comparison of the analytic and the numeric optimization under efficiency-optimized concentration. The colors distinguish different extrinsic absorber resistances ρ_a. Broad dashed lines: Analytical results for the area fractions of the electron contact f_e (top left graph) and the hole contact f_h (top right graph) from Equation (29), the concentration C (bottom left graph) from Equations (25) and (22), and the efficiency η (bottom right graph) from Equation (15). Narrow dash-dotted lines: numeric optimization. Dotted lines: numeric optimization with the injection-dependent intrinsic resistance of the absorber. The parameters are identical to those given in the caption of Figure 2.

are approximations. In consistency with ref. [4], the analytic efficiency η is slightly larger than the numeric result. Again we find a difference of about $0.08\%_{abs}$ efficiency points. The dotted line is again a numerical optimization accounting for the injection-dependent intrinsic wafer resistance.

For all numeric results in Figures 2 and 3, we observe numeric convergence to a maximum efficiency. This is worth mentioning as we did not explicitly prove that the analytic solutions describe an efficiency maximum rather than a minimum or a saddle point. In Figure 2, the analytic efficiency for $\rho_a = 10\,\mathrm{m\Omega\,cm^2}$ under 1 sun (broad dashed black line) drops from 27.6% at

$J_a = 1\,\mathrm{fA\,cm^{-2}}$ to 24.2% at $J_a = 100\,\mathrm{fA\,cm^{-2}}$. Under optimized concentration, this efficiency drops in Figure 3 over the same range of recombination currents J_a from a slightly higher value of 28.0% at $C = 7$ to a significantly higher value of 26.6% at $C = 35$, when compared to the non-concentrating case. The enhancement form 24.2 to 26.6% is due to the iso-selectivity scaling of a device with a low resistances and high recombination. Figure 3 also shows that in the opposite case of low recombination J_a and high resistances, the iso-selectivity scaling works in the opposite direction and optimizes the efficiency by de-concentrating the light intensity to $C < 1$.

In Figures 2 and 3, the dotted lines for a Si absorber with its intrinsic injection-dependent wafer resistance are close to those for $\rho_a = 10\,\text{m}\Omega\text{cm}^2$, in particular at low J_a values of 1 to $100\,\text{fA cm}^{-2}$. Please note that a wafer with specific resistance $r_{\text{bulk}} = 1\,\Omega\text{cm}$ and a thickness $W = 100\,\mu\text{m}$ would contribute in low injection $r_{\text{bulk}}W = 10\,\text{m}\Omega\text{cm}^2$ to the total resistance. This order of magnitude is thus to be expected for the absorber resistance of an efficient Si cell. From the dotted C line in Figure 3, we find that POLO type of cells with a poor material quality $J_a = 100\,\text{fA cm}^{-2}$ and with the contacts as the only sources of extrinsic resistances would still allow for high efficiencies of up to 26.0% if the cell is put under high concentration of $C = 47$.

4. Summary

In the framework of a single-diode model, we derived a set of equations for an efficiency-optimized solar cell with electron contacts (ρ_e, J_e), hole contacts (ρ_h, J_h), and given absorber properties (ρ_a, J_a). If light concentration is allowed, we first optimize the contact fractions f_e and f_h for optimal selectivity and then put the device under optimum concentration C. The second step can be described as inverse scaling of recombination rates against transport resistance under the constraint of constant device selectivity. If light concentration is not allowed, the optimum efficiency is achieved at less-than-optimum device selectivity. For this case, we also gave analytic expressions. In the admittedly limited range of validity of the one-diode model, the analytic and numeric optimization gives similar results for all tests conducted. Our novel analytic equations may thus be used to easily estimate optimal efficiencies, optimal contact fractions, and the optimal solar concentration. We applied these equations to the special case of POLO cells that combine local screen-printed hole contacts with n-type poly-silicon contacts and calculated the dependence of the optimum concentration level on the recombination parameter J_a of the bulk for various series resistances ρ_a. High efficiencies of up to 26.0% are theoretically feasible even with rather high recombination of $J_a = 100\,\text{fA cm}^{-2}$ if the cell is put under optimal concentration and has negligible extrinsic resistances.

[1] R. Brendel, C. Kruse, A. Merkle, H. Schulte-Huxel, F. Haase, R. Peibst, in *Proc. 35th European Photovoltaic Solar Energy Conf.*, WIP-Renewable Energies, Brussels **2018**, pp. 39–46.

[2] R. Brendel, M. Rienaecker, R. Peibst, in *Proc. 32nd European Photovoltaic Solar Energy Conf.*, WIP Renewable Energies, Munich **2016**, pp. 447–451.

[3] B. Min, N. Wehmeier, T. Brendemuehl, F. Haase, Y. Larionova, L. Nasebandt, H. Schulte-Huxel, R. Peibst, R. Brendel, *Sol. RRL* **2021**, 5, 2000703.

[4] U. Rau, T. Kirchartz, *Adv. Mater. Interfaces* **2019**, 6, 1900252.

[5] R. Brendel, R. Peibst, *IEEE J. Photovoltaics* **2016**, 6, 1413.

[6] C. N. Kruse, S. Schüafer, F. Haase, V. Mertens, H. Schulte-Huxel, B. Lim, B. Min, T. Dullweber, R. Peibst, R. Brendel, *Sci. Rep.* **2021**, 11, 996.

[7] D. T. Cotfas, P. A. Cotfas, S. Kaplanis, *Renewable Sustainable Energy Rev.* **2013**, 28, 588.

[8] S. Schafer, R. Brendel, *IEEE J. Photovoltaics* **2018**, 8, 1156.

[9] M. A. Green, *Solid-State Electron.* **1981**, 24, 788.